JOURNAL OF SOLID STATE CHEMISTRY 104, 81–87 (1993)

Synthesis and Characterization of Ni_3S_2 Single Crystals

P. A. METCALF, P. FANWICK, Z. KĄKOL,* AND J. M. HONIG

Department of Chemistry, Purdue University, West Lafayette, Indiana 47907-1393

Received October 29, 1992; accepted November 9, 1992

The synthesis and growth of single crystals of Ni_3S_2 are described. Structural information is provided on the room-temperature configuration of this compound. Measurements of electrical resistivity, magnetic susceptibility, and heat capacity below room temperature have been carried out and are briefly discussed. The material may be classified as a good metallic conductor.

Introduction

Nickel sulfide, Ni_3S_2, occurs naturally as the mineral heazlewoodite. The structure, originally proposed by Westgren (*1*), and more recently refined by Fleet (*2*) and Parise (*3*), is rhombohedral; it belongs to the space group $R32$, with lattice constants $a_r = 4.071$ Å, $\alpha_r = 89.459°$, and $Z = 1$. The structure comprises a series of interconnected Ni_3S_2 regular bipyramids composed of Ni_3 triangles and apical S atoms. These units are interconnected by short Ni–S and Ni–Ni distances, the distances between atoms within the bipyramids being greater than those connecting the bipyramids (*3*) (see Fig. 1). This structure occurs as the low temperature form of Ni_3S_2 and is known to be stable up to 843 K. The phase diagram for Ni–S, reproduced in Fig. 2, was originally constructed by Kullerud and Yund (*5*) and later modified by Lin *et al.* (*6*). Above 843 K, Ni_3S_2 undergoes a transition to the cubic high-temperature phase, $Ni_{3+x}S_2$, which melts incongruently above 800°C.

Almost all of the physical measurements reported for Ni_3S_2 have been performed either on the naturally occurring mineral or on polycrystalline samples at temperatures greater than 290 K. As part of an ongoing study of nickel sulfide and related systems, single crystals of Ni_3S_2 were grown in this laboratory and their magnetic and transport properties were measured at and below room temperature. We concentrate here on the details of the preparation and characterization, and we also briefly report the initial results of the physical measurements.

Experimental

A. Preparation and Characterization of Samples

Samples of microcrystalline Ni_3S_2 were prepared by the reduction of $NiSO_4$ in hydrogen. Approximately 50 grams of $NiSO_4 \cdot 3H_2O$ were placed in a nickel foil-lined alumina boat and heated to 120°C to form the anhydrous material. The boat was

* Permanent address: Zakład Fizyki Ciała Stałego IM, Akademia Gorniczo-Hutnicza, 30-059 Krakow, Poland.

0022-4596/93 $5.00

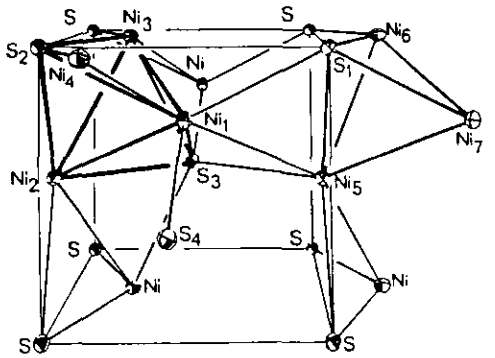

FIG. 1. ORTEP drawing of Ni_3S_2 (*4*). Labels refer to Tables II and III. A Ni_3S_2 bipyramid is outlined.

then transferred to a hydrogen furnace, heated at 500°C for 2 hr, and furnace-cooled. The resulting green powder was analyzed by X-ray powder diffraction, using a Siemens DIFF500 diffractometer with CuK_α radiation. The powder pattern coincided with previously reported results for Ni_3S_2; no other phases were detected. Shorter heating times resulted in material with excess elemental sulfur, while much longer heating times led to the reduction of Ni_3S_2 to nickel metal.

Very dense polycrystalline samples of Ni_3S_2 were obtained by a "melt–quench" technique. Stoichiometric amounts of 99.999% pure nickel and sulfur powders were placed in a silica tube, which was constricted above the charge but not sealed. The tube and charge were heated in a hydrogen/oxygen flame until convection currents were observed within the melt. The tube was then removed from the flame and quenched in water. The resulting boule was metallic bronze in appearance. Analysis by EDAX showed the material to be sulfur-deficient, with the nickel to sulfur ratio of 1.61 (±0.01) Ni to 1.00 (±0.01) S. Within the error of the EDAX measurements, no contamination was detected and the sample composition was found to be homogenous. No nickel or sulfur inclusions were observed via optical microscopy using polarized light. The X-ray diffraction patterns of these specimens again coincided with that for Ni_3S_2. No extraneous phases were detected in the diffractograms; see Table I.

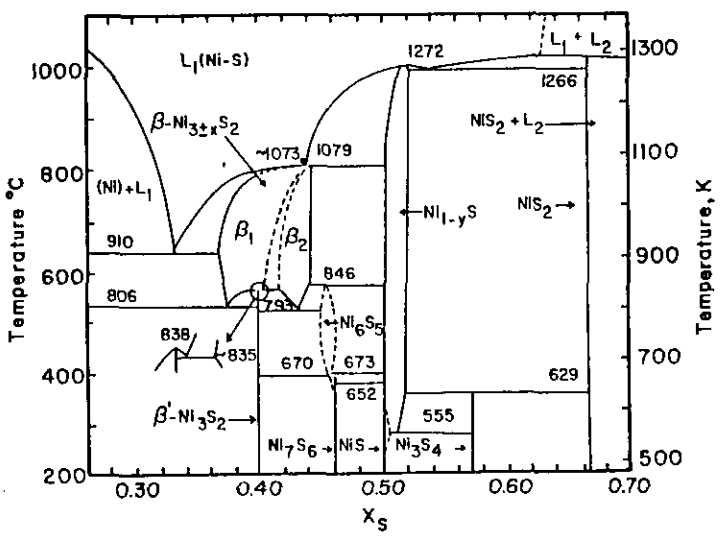

FIG. 2. Nickel–sulfur phase diagram, after Lin *et al.* (*6*). β'-Ni_3S_2 is the low temperature form, while β_1 and β_2 are the nickel- and sulfur-rich high temperature $Ni_{3\pm x}S_2$ phases.

TABLE I

X-RAY POWDER DATA FOR Ni_3S_2 *R*32, RHOMBODEDRAL $a_r = 4.0821$, $\alpha_r = 89.475(9)°$, $Z = 1$

	2θ			I/I_0		
h k l	calc	obs[a]	obs[b]	calc	obs[a]	obs[b]
1 0 1	21.76	21.74	21.72	69	99	59
1 1 0	31.10	31.11	31.09	100	100	100
0 0 3	37.80	37.79	37.78	36	34	37
0 2 1	38.28	38.28	38.29	12	23	14
2 0 2	44.36	44.36	44.36	37	77	40
1 1 3	49.72	49.72	49.72	52	74	51
2 1 1	50.12	50.12	50.10	45	65	34
1 0 4	54.62	54.59	54.62	18	22	16
1 2 2	55.16	55.15	55.20	59	84	54

[a] Single crystals.
[b] Polycrystalline.

Single crystals of Ni_3S_2 were grown by a vapor transport technique. Microcrystalline Ni_3S_2 obtained from the reduction of $NiSO_4$ was loaded into one end of a nickel-lined alumina boat, which was then positioned in a three-zone horizontal tube furnace. A second fused silica boat containing 99.999% pure sulfur was positioned at the opposite end of the furnace. The furnace tube was equipped with end-caps which allowed nitrogen to flow through the tube during heating. The silica boat containing sulfur was maintained at 200°C; the end of the alumina boat containing the Ni_3S_2 powder was maintained at ~750°C while the opposite end of the boat was at a lower temperature, as shown in Fig. 3. Nitrogen gas was circulated through the tube for several hours prior to heating, and the flow was maintained at a rate of approximately 100 ml/min during crystal growth. The furnace was held at the indicated temperature profile for about 48 hr and was then allowed to cool to room temperature in flowing nitrogen.

Crystals of Ni_3S_2 formed on the nickel liner at the cool end of the boat. The crystals were brass-yellow prisms, with dimensions up to 2 mm on an edge. One of the smaller prisms was chosen for an X-ray diffraction study. The refinement confirmed the structure of the crystals to be that reported for heazlewoodite (*2, 3*) (Tables II and III). The nickel to sulfur ratio of the crystals as examined by electron microprobe analysis was found to be 1.49 (±0.01) Ni to 1.00 (±0.01) S. The crystals were also examined by transmission electron microscopy. The [100] electron diffraction pattern and [100] HRTEM image obtained from large pieces of two crushed single crystals are shown in Fig. 4. One square in the HRTEM image corresponds to a unit cell of Ni_3S_2 with edges *b* and *c*. The TEM results show no short range defects or disorder in the areas examined.

B. Electrical Conductivity Measurements

The electrical conductivity was measured for a single Ni_3S_2 crystal using the four-probe van der Pauw method. The dimensions of the crystal were approximately 0.3 × 0.3 × 0.1 mm. The contacts were formed by evaporating silver metal pads, onto which copper wires were attached with silver paint. The distance between the contacts was 0.1 mm. A Keithley Model 224 programmable current source was used and the voltage drop across the sample was mea-

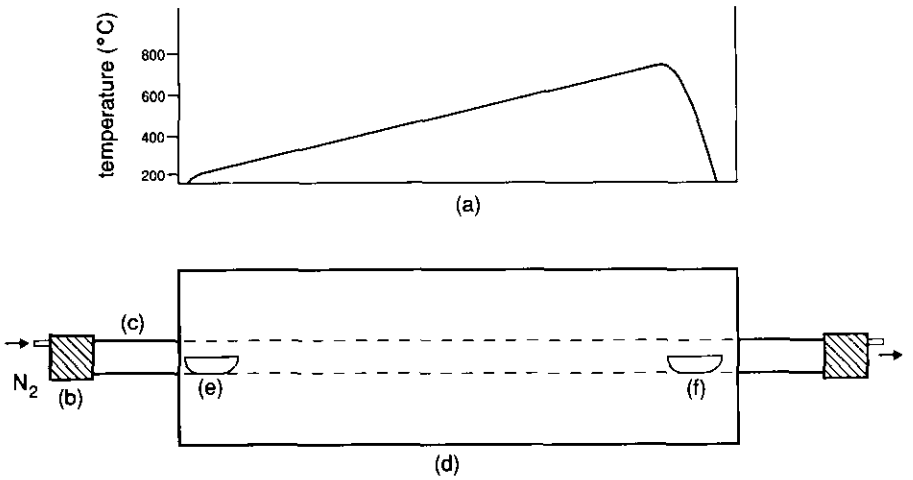

FIG. 3. Experimental apparatus for crystal growth; see text. (a) Approximate furnace profile, (b) end-caps for atmosphere control, (c) alumina furnace tube with quartz tube liner, (d) three-zone horizontal furnace, (e) fused silica boat with sulfur, and (f) alumina boat with Ni_3S_2.

sured by a Keithley Model 181 nanovoltmeter. The current employed in the experiment was 20 mA. The conductivity was measured as a function of temperature between 300 K and 4.5 K. The sample temperature was monitored with a calibrated carbon-gas thermocouple and controlled with a Lake Shore Cryotonics model DRC 91C temperature controller. The data collection was computerized.

C. Magnetic Susceptibility Measurements

The magnetic susceptibility was measured for the Ni_3S_2 crystals and polycrystalline samples by two methods. In one technique the magnetic data were obtained from 300 K to 4.5 K using a Princeton Applied Research vibrating sample magnetometer (VSM) utilizing field strengths between 5 Oe and 6 kOe. A Quantum Design SQUID magnetometer was used to collect data from 350 K to 10 K at field strengths between 1 and 55 kOe. Due to the large uncertainty in the magnitude of the correction relative to the measured susceptibility, no core diamagnetic correction was applied to the measurements.

Results and Discussion

We briefly discuss the experimental findings:

A. Conductivity

The temperature dependence of the electrical resistivity for a single crystal of Ni_3S_2 is shown in Fig. 5. The sample exhibited metallic behavior over the entire range from 300 K to 4.5 K. The room temperature resistivity for the crystal was approximately $\rho = 1.8 \times 10^{-5}$ Ω-cm, which is lower by one order of magnitude than that reported for polycrystalline samples (*6*). At 4.2 K the resistivity value had dropped to $\rho = 2 \times 10^{-7}$ Ω-cm; the resistivity ratio of approximately 100 indicates that the single crystal is reasonably perfect. Measurements on samples of the melt-quenched polycrystalline material showed a similar metallic temperature dependence, with a room tempera-

TABLE II

DISTANCES (Å) AND ANGLES (°) IN Ni_3S_2

	This work	Ref (a)	Ref (b)	Ideal
Ni(1)–S(1)	2.255	2.27	2.2534	2.28
Ni(1)–S(2)	2.295	2.27	2.2914	2.28
Ni(1)–S(3)	2.295	2.27	2.2914	2.28
Ni(1)–S(4)	2.255	2.27	2.2534	2.28
Ni(1)–Ni(2)	2.539	2.52	2.5319	2.50
Ni(1)–Ni(3)	2.539	2.52	2.5319	2.50
Ni(1)–Ni(4)	2.501	2.51	2.4966	2.50
Ni(1)–Ni(5)	2.501	2.51	2.4966	2.50
S(1)–S(2)	4.08	4.0821	4.0718	4.08
S(1)–S(3)	3.51	3.50	3.5051	3.54
S(1)–S(4)	3.53	3.50	3.5255	3.54
S(2)–S(3)	3.53	3.55	3.5291	3.54
S(1)–Ni(1)–S(2)	127.3	127.8	127.25	126.9
S(1)–Ni(1)–S(3)	100.9	100.7	100.92	101.5
S(1)–Ni(1)–S(4)	103.1	102.6	102.94	101.5
S(2)–Ni(1)–S(3)	100.6	100.6	100.72	101.5
Ni(2)–Ni(1)–Ni(3)	60.0	60.0	60.0	—
Ni(2)–Ni(1)–Ni(4)	98.9	99.2	98.95	—
Ni(2)–Ni(1)–Ni(5)	108.0	108.6	108.13	—
Ni(3)–Ni(1)–Ni(4)	108.0	108.6	108.13	—
Ni(4)–Ni(1)–Ni(5)	148.9	147.9	148.73	—
S(2)–Ni(1)–Ni(4)	55.9	—	55.95	—
S(1)–Ni(1)–Ni(4)	101.8	—	101.71	—
S(1)–Ni(1)–Ni(3)	99.9	—	99.93	—
S(1)–Ni(1)–Ni(2)	154.9	—	155.04	—
S(4)–Ni(1)–Ni(4)	57.4	—	57.41	—
Ni(5)–S(2)–Ni(6)	67.2	67.2	67.07	—
Ni(1)–S(1)–Ni(6)	114.6	112.6	114.51	—
Ni(1)–S(1)–Ni(7)	127.3	—	127.25	—
Ni(1)–S(1)–Ni(5)	66.7	67.0	66.64	—

[a] M.E. Fleet (*2*).
[b] J.B. Parise (*3*).

TABLE III

FRACTIONAL ATOMIC COORDINATES

	x			*y*			*z*		
	This work	Ref. (*a*)	Ref. (*b*)	This work	Ref. (*a*)	Ref. (*b*)	This work	Ref. (*a*)	Ref. (*b*)
Ni	.5	.5	.5	.2555	.247	.2449	.7445	.753	.7551
S	.2475	.255	.2521	.2475	.255	.2521	.2475	.255	.2521

[a] M.E. Fleet (*2*).
[b] J.B. Parise (*3*).

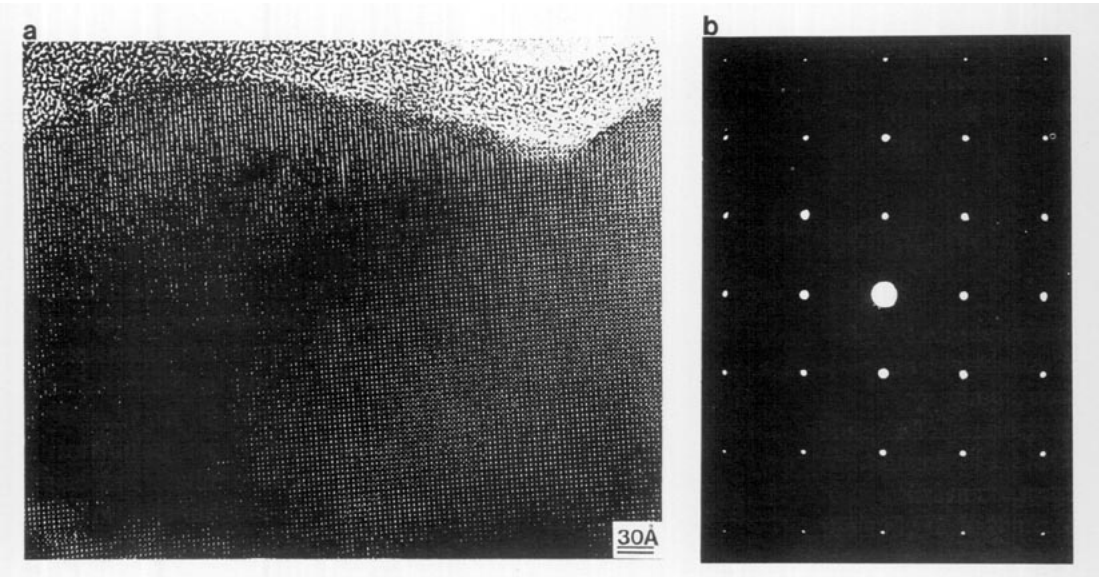

FIG. 4. TEM photographs of Ni_3S_2 crystals. (a) High resolution TEM image [100]; one square in image corresponds to a unit cell with edges b and c. (b) Electron diffraction pattern [100].

ture resistivity value of approximately 1.2×10^{-4} Ω-cm, which is comparable to that previously reported in the literature for polycrystalline samples (*8*).

B. Magnetic Susceptibility

The magnetic susceptibility for the Ni_3S_2 crystals at temperatures from 300 K to 4.5 K and for fields up to 55 kOe was found to be essentially field- and temperature-independent. The susceptibility value of $\chi = 0.3 \times 10^{-6}$ emu/g is nearly identical with that reported for polycrystalline material (*7*). These results are consistent with Pauli paramagnetism of the type encountered in ordinary metals.

C. Heat Capacity

Heat capacity measurements for the polycrystalline samples were carried out by the quasi-adiabatic heat pulse method in the temperature range from 150 K down to 0.5 K. No major heat-capacity anomalies were observed in the measured temperature range. In the lower temperature region, $T <$ 6 K, the heat capacity was fitted by assuming a linear $C_p/T = \alpha T^2 + \gamma$ relation. The values of $\alpha = 0.15$ mJ/mol, $\gamma = 8.4$ mJ/mol K^2, and $\theta_D = 398$ K were obtained. These findings stand in sharp contrast to the result by Stølen *et al.* (*9*) who, by extrapolation, obtained an electronic heat capacity constant $\gamma = 0$. The γ values ascertained in this study are representative of electronic contributions anticipated for conventional metals.

Conclusion

Single crystals of Ni_3S_2 were grown by a vapor transport technique, and polycrystalline samples were prepared using a melt–quench method. The samples were characterized by single crystal and powder X-ray diffraction, microprobe analysis,

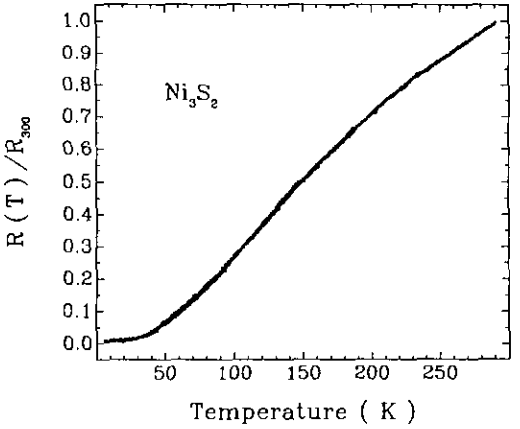

FIG. 5. Temperature dependence of resistivity for a single crystal of Ni_3S_2.

EDAX, and TEM. Measurements of the dc resistivity, magnetic susceptibility, and heat capacity indicate that the material is a reasonably good metallic conductor. More detailed physical measurements are planned for the future.

Acknowledgments

We thank B. C. Crooker, M. McElfresh, and N. Otsuka for their contributions to this investigation. This research was supported in part by MISCON at Purdue University on Grant DE-FG02-90ER45427, and in part by ACS-PRF Grant 22396-AC3-C.

References

1. A. Z. WESTGREN, *Z. Anorg. Allg. Chem.* **82,** 239 (1938).
2. M. E. FLEET, *Am. Mineral.* **62,** 341 (1977).
3. J. PARISE, *Acta Crystallogr. Sect. B* **36,** 1179 (1980).
4. C. K. JOHNSON, ORTEP, Report ORNL-3794, Oak Ridge National Laboratory, Tennessee (1965).
5. G. KULLERUD AND R. A. YUND, *J. Petrol.* **3,** 126 (1962).
6. R. Y. LIN, D. C. HU, AND Y. A. CHANG, *Metall. Trans. B* **9,** 531 (1978).
7. D. M. PASQUARIELLO, R. KERSHAW, J. D. PASSARETTI, K. DWIGHT, AND A. WOLD, *Inorg. Chem.* **23,** 872 (1981).
8. H. YAGI AND J. B. WAGNER, JR., *Oxid. Met.* **19,** 41 (1982).
9. S. STØLEN, F. GRØNVOLD, E. WESTRUM, JR., AND G. KOLONIN, *J. Chem. Thermodyn.* **23,** 77 (1991).